$P\bar{6}m2$-ReB_3的高压物性研究

雷慧茹，张立宏
(山西工程技术学院基础教学部，阳泉 045000)

摘　要：本文利用赝势平面波法计算了 ReB_3 的三种晶体结构 $P\bar{6}m2$，$P6_3/mmc$ 及 $P\bar{3}m1$ 的结构属性. 研究发现 $P\bar{6}m2$-ReB_3 是 ReB_3 的基态相位. 我们首次系统研究了高压下 $P\bar{6}m2$-ReB_3 的弹性常数、弹性各向异性、各种弹性模量及波速度等弹性特性，并且预测了 $P\bar{6}m2$-ReB_3 的韧脆性. 此外，通过准谐德拜模型，我们还分析了 $P\bar{6}m2$-ReB_3 结构的德拜温度、标准化体积、体积模量、热膨胀系数及热容与压力或温度的依赖关系.

关键词：ReB_3；高压；结构属性；弹性性质；热力学性质
中图分类号：O521+.2/O414　　**文献标识码**：A　　DOI：10.19907/j.0490-6756.2022.014004

High-pressure physical properties for $P\bar{6}m2$-ReB_3

LEI Hui-Ru, *ZHANG Li-Hong*
(Department of Basic Subjects Teaching, Shanxi Institute of Technology, Yangquan 045000, China)

Abstract: In this paper, three crystal structures of ReB_3, $P\bar{6}m2$, $P6_3/mmc$, $P\bar{3}m1$, and their structural properties, are calculated by using pseudopotential plane-wave method. It is found that the $P\bar{6}m2$-ReB_3 is the ground-state phase of ReB_3. In particular, the elastic properties such as, elastic constants, elastic anisotropy, aggregate moduli and wave velocities of $P\bar{6}m2$-ReB_3 under high pressure are investigated systematically for the first time. The toughness and brittleness are also predicted for the $P\bar{6}m2$-ReB_3 structure. In addition, dependences of the Debye temperature, normalized volume, bulk modulus, thermal expansion coefficient, and heat capacity on pressure or temperature for the $P\bar{6}m2$-ReB_3 structure are analyzed through the quasi-harmonic Debye model.

Keywords: ReB_3; High pressure; Structural features; Elastic properties; Thermodynamic properties

1　Introduction

Recent years, transition metal compounds have aroused extensive attentions due to their superiorphysical properties and potential application value[1-4]. As one of the 5d transition metals, Rhenium has a considerable bulk modulus (360～372 GPa), but a comparatively low shear modulus (179 GPa)[5,6]. When it is inserted the light element B, C, or N, the highly oriented covalent bonds have formed, so the Re-B/C/N systems are explored by many scientists[7-9]. In the Re-B system, rhenium triborides (ReB_3) was firstly synthesized with hexagonal $P6_3/mmc$ structure in 1960[10], but Gou *et al*.[11] and Zhao *et al*.[12] reported it to be thermodynamically unstable with

收稿日期：2021-07-24
基金项目：山西工程技术学院校级科研基金(2021001)
作者简介：雷慧茹(1988－)，女，山西阳泉人，主要研究领域为高硬度材料的高压物性. E-mail: leihuiru1988@163.com

the positive formation enthalpy. In 2014, using the genetic algorithms, Zhao *et al.*[13] obtained ReB_3 to be stable above 22 GPa in another hexagonal $P\bar{6}m2$ structure. Subsequently, the $P\bar{6}m2$ structure was also successfully predicted by using the Crystal structure Analysis by Particle Swarm Optimization (CALYPSO) method, and a new $P6_3/mmc$ structure which has shorter Re-B and B-B bond than previous studies[10-12] was found at the same time[14]. Both the structures were calculated thermodynamically stable at 0 GPa. The $P\bar{6}m2$ structure was predicted to be the ground-state phase under the pressure in a range of 0～100 GPa. Meanwhile, ReB_3 in the trigonal $P\bar{3}m1$ structure was estimated thermodynamically stable above 5 GPa. Therefore, in this work, ReB_3 in three structures are considered, hexagonal $P\bar{6}m2$ (No. 187), $P6_3/mmc$ (No. 194) (the one in Ref. [14]) structures and trigonal $P\bar{3}m1$ (No. 164) structure.

In addition, the elastic constants of a solid are necessary because they are not only closely linked with some fundamental solid-state characteristics, but also correlated with many thermodynamic properties. Most importantly, various mechanical properties are associated with the elastic constants which are indispensable for the practical applications[15]. Hitherto several studies have calculated the elastic constants of ReB_3 at 0 GPa[13,14], but the elastic constants of ReB_3 at high pressure have rarely been reported.

The subject of this paper is to investigate the structural, elastic and thermodynamic properties of ReB_3 under high pressure by using the pseudopotential plane-wave methods within the density functional theory. In the following, our theoretical methods, results and discussion are presented in detail.

2 Computational detail

2.1 Electronic structure calculations

Our geometry optimization, total energy calculations and phonon calculations are implemented through the CASTEP code[16], based on the plane-wave pseudopotential density function theory (DFT). The Vanderbilt ultrasoft pseudopotentials[17] are generated by the generalized gradient approximation of Perdew *et al.* (GGA-PBE)[18,19]. In the structure calculation, the kinetic energy cutoff is set to 500 eV, the k-points sampling for Brillouin-zone are set to $10 \times 10 \times 6$ which are selected by using the Monkhorst-Pack method[20]. With above parameters, the self-consistent convergence of the total energy can achieve less than 1×10^{-6} eV/cell. In phonon calculations, the interatomic force constant is calculated by using a supercell approach with the finite displacement method, and the supercell size for ReB_3 is $1 \times 1 \times 1$ in the calculations. In addition, the initial structures for $P\bar{6}m2$, $P6_3/mmc$ and $P\bar{3}m1$ before optimization are from Ref. [14].

2.2 Elastic constants

When a material is subjected to an external force within its elastic limit, the elastic constants C_{ijkl} under hydrostatic pressure can be obtained by the coefficients connecting the applied stress σ_{ij} and the Eulerian strain tensors e_{kl} as follows[21,22]:

$$C_{ijkl} = \left(\frac{\partial \sigma_{ij}(X)}{\partial e_{kl}}\right)_x \tag{1}$$

where X and x represent the coordinates before and after the deformation, respectively. For an isotropic stress, the specific formulas are[22,23]:

$$C_{ijkl} = c_{ijkl} + \frac{p}{2}(2\delta_{ij}\delta_{kl} - \delta_{il}\delta_{jk} - \delta_{ik}\delta_{jl}) \tag{2}$$

$$c_{ijkl} = \left(\frac{1}{V(x)}\frac{\partial^2 E(x)}{\partial e_{ij}\partial e_{kl}}\right)_x \tag{3}$$

where c_{ijkl} denotes the second-order derivative of the infinitesimal Eulerian strain. The strains used are non-volume conserving. Moreover, the number of fourth-rank tensor C is closely related to the symmetry of the crystal. For a hexagonal crystal, the fourth-rank tensor C has five independent components C_{11}, C_{33}, C_{44}, C_{12} and C_{13}.

2.3 Thermodynamic properties

The quasi-harmonic Debye model[24] has been successfully investigated the thermodynamic

properties of some materials (*i. e.* TiB_2[25], GaN[26] and YbB_6[27]). To compute the thermodynamic properties of ReB_3, the GIBBS program within the quasi-harmonic Debye model[24] is employed, where the non-equilibrium Gibbs function $G^*(V; p, T)$ can be expressed as:

$$G^*(V;p,T)=E(V)+pV+A_{vib}(\Theta(V);T) \tag{4}$$

where $\Theta(V)$ is the Debye temperature, A_{vib} is the vibrational term which takes the form:

$$A_{vib}(\Theta;T)=nkT\left[\frac{9}{8}\frac{\Theta}{T}+3\ln(1-e^{\Theta/T})-D(\Theta/T)\right] \tag{5}$$

where n is the number of atoms in a primitive cell, $D(\Theta/T)$ is the Debye integral. The thermal expansion coefficient α can be obtained from[24]:

$$\alpha=\frac{\gamma C_V}{B_T V} \tag{6}$$

where γ, B_T, C_V and C_p stand for Grüneisen parameter, isothermal bulk modulus, heat capacity at constant volume, and heat capacity at constant pressure, respectively. The related formulas are[24]:

$$\gamma=-\frac{\mathrm{d}(\ln\Theta(V))}{\mathrm{d}(\ln(V))} \tag{7}$$

$$B_T(p,T)=V\left(\frac{\partial^2 G^*(V;p,T)}{\partial V^2}\right)_{p,T} \tag{8}$$

$$C_V=3nk\left[4D(\Theta/T)-\frac{3\Theta/T}{e^{\Theta/T}-1}\right] \tag{9}$$

$$C_p=C_V(1+\alpha\gamma T) \tag{10}$$

3 Results and discussion

3.1 Structural features

At a micro level, structural properties can provide valuable information about the character of the inter-atomic binding forces between atoms in solids. The structural properties of ReB_3 in the P$\bar{6}$m2, $P6_3$/mmc, and P$\bar{3}$m1 structures are investigated by using the first-principles calculations. In order to get the variations of the total energy E with corresponding primitive cell volume V of ReB_3, we have done geometry optimization for different pressures. The calculated E-V points are fitted to the Birch-Murnaghan equation of state[28], then the lattice constants a and c, the equilibrium volume V_0, and the bulk modulus B_0 at 0 K are obtained (listed in Tab. 1). We note that our calculated values are consistent with previous theoretical values[13,14], and show the accuracy of our electronic structure calculations.

Tab. 1　Lattice constants a, c, equilibrium volume V_0, and bulk moduli B_0 for ReB_3 structures at 0 K and 0 GPa

Phase	Results	a/Å	c/Å	V_0/Å^3	B_0/GPa
P$\bar{6}$m2-ReB_3	This work	2.921	4.582	33.85	313
	Ref. [14]	2.924	4.595	34.01	320
	Ref. [13]	2.920	4.590	34.01	
$P6_3$/mmc-ReB_3	This work	2.917	9.434	69.53	313
	Ref. [14]	2.904	9.313	68.04	
P$\bar{3}$m1-ReB_3	This work	2.874	4.667	33.40	303
	Ref. [14]	2.874	4.673	33.44	

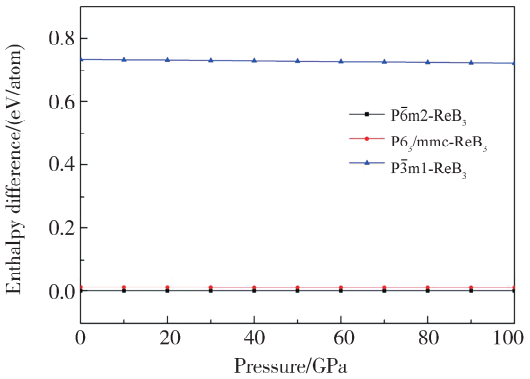

Fig. 1　The enthalpy differences for P$\bar{6}$m2, $P6_3$/mmc, P$\bar{3}$m1 structures with respect to P$\bar{6}$m2 structure as a function of pressure at 0 K

As is well-known, the thermodynamic stable structure has the lowest Gibbs free energy G which equals to the enthalpy H for solid at 0 K, *i. e.*, $G=H=E+pV$, where $p=-\partial E/\partial V$. Fig. 1 shows the enthalpy differences as a function of pressure. We can see that, P$\bar{6}$m2-ReB_3 has the smallest enthalpy which indicates the P$\bar{6}$m2-ReB_3 to be the ground-state phase, and the result is well consistent with Zhao *et al.*[13] and Yan *et al.*[14]. Dynamically, the calculated phonon dispersion curves (Fig. 2) also conform the dynamical stability of P$\bar{6}$m2-ReB_3 at 0 GPa and under high pressure.

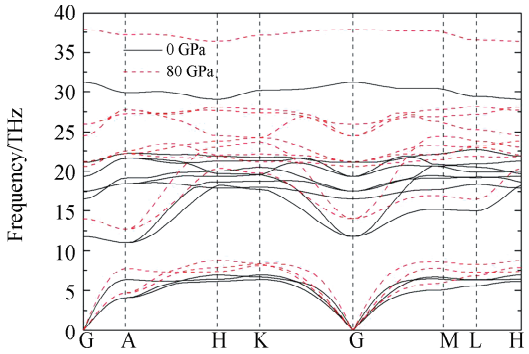

Fig. 2　Calculated phonon dispersion relations for the $P\bar{6}m2$-ReB_3 structure

3.2　Elastic properties

The elastic constants of $P\bar{6}m2$-ReB_3 at 0 K and 0 GPa are summarized in Tab. 2. It is found that the agreement between our results and other theoretical values[13,14] is good. To judge the mechanical stability of $P\bar{6}m2$-ReB_3, we can substitute the elastic constants into the generalized criteria for hexagonal crystal:

$$C_{44}>0, C_{11}>|C_{12}|, (C_{11}+2C_{12})C_{33}>2C_{13}^2 \tag{11}$$

Apparently, all above conditions are satisfied, indicating the mechanical stability for $P\bar{6}m2$-ReB_3 structure at 0 K and 0 GPa. Furthermore, we have also investigated the mechanical stability under high pressure, and the elastic constants of $P\bar{6}m2$-ReB_3 as functions of the pressure are plotted in Fig. 3. It is found that C_{11} and C_{33} are susceptible to pressure where as C_{12}, C_{13} and C_{44} are less affected by pressure. This is because C_{11} and C_{33} express the elasticity in length and can be influenced by the longitudinal strain whereas C_{12}, C_{13} and C_{44} signify the elasticity in shape and can be affected by the transverse strain[29].

Tab. 2　Elastic constants C_{ij}, Bulk modulus B, shear modulus G, the ratio of B/G, Young's modulus E, Poisson's ratio σ, and Debye temperature Θ of $P\bar{6}m2$-ReB_3

Results	C_{11}/GPa	C_{33}/GPa	C_{44}/GPa	C_{12}/GPa	C_{13}/GPa	B/GPa	G/GPa	B/G	E/GPa	σ	Θ/K
This work	600	902	212	104	167	323	240	1.34	577	0.20	773
Ref. [14]	567	905	229	130	175	333	239	1.39	579	0.21	764
Ref. [13]	575	911	223	140	181	332	235	1.41	570	0.21	

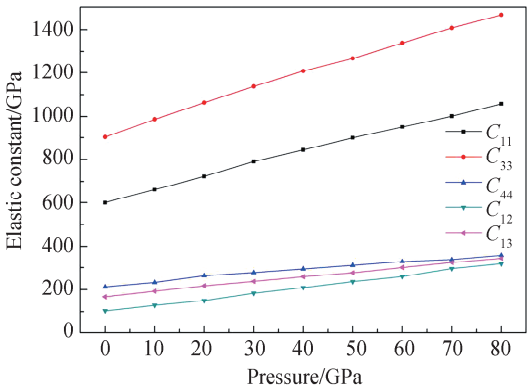

Fig. 3　Variations of elastic constants with pressure for the $P\bar{6}m2$-ReB_3 structure

Three types of elastic waves about the elastic anisotropy of the hexagonal $P\bar{6}m2$-ReB_3 under high pressure can be calculated by the above elastic constants[30]:

$$\Delta p=\frac{C_{33}}{C_{11}} \tag{12}$$

$$\Delta S_1=\frac{(C_{11}+C_{33}-2C_{13})}{4C_{44}} \tag{13}$$

$$\Delta S_2=\frac{2C_{44}}{C_{11}-C_{12}} \tag{14}$$

where Δp, ΔS_1, and ΔS_2 are the anisotropies of the compressional wave and two shear waves, respectively. In Fig. 4, we illustrate the elastic anisotropic parameters as functions of the pressure. Noting that the Δp, ΔS_1 show a gradual decline while ΔS_2 behaves a moderate rise in the range of applied pressures. This indicates the elastic anisotropy of $P\bar{6}m2$-ReB_3 under high pressure, and the phenomena may be understood by comparison to a hexagonal crystal interacting with central nearest-neighbor forces CNNF[31]. For this model, the elastic anisotropy is independent of the interatomic potential to lowest order in p/C_{11}, so the anisotropy depends only on the symmetry of the crystal.

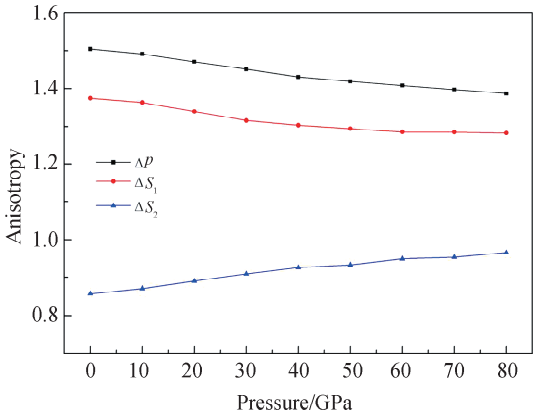

Fig. 4　The elastic anisotropic parameters versus pressure for the P$\bar{6}$m2-ReB_3 structure

It is well-known that the hardness can be predicted by the bulk modulus B and the shear modulus G. The Voigt-Reuss-Hill average scheme[32] introduces the methods to calculate the crystal modulus:

$$B=\frac{1}{2}(B_V+B_R) \tag{15}$$

$$G=\frac{1}{2}(G_V+G_R) \tag{16}$$

For a hexagonal structure, the B_V, B_R, G_V, and G_R are given as:

$$B_V=\frac{1}{9}[2(C_{11}+C_{12})+4C_{13}+C_{33}], \tag{17}$$

$$B_R=\frac{(C_{11}+C_{12})C_{33}-2C_{13}^2}{C_{11}+C_{12}+2C_{33}-4C_{13}} \tag{18}$$

$$G_V=\frac{1}{30}(C_{11}+C_{12}+2C_{33}-4C_{13}+12C_{44}+12C_{66}) \tag{19}$$

$$G_R=\frac{5}{2}\cdot\frac{[(C_{11}+C_{12})C_{33}-2C_{13}^2]C_{44}C_{66}}{3B_VC_{44}C_{66}+[(C_{11}+C_{12})C_{33}-2C_{13}^2](C_{44}+C_{66})} \tag{20}$$

where

$$C_{66}=\frac{1}{2}(C_{11}-C_{12}) \tag{21}$$

The Young's modulus E and Poisson's ratio σ can be obtained from the following equations:

$$E=\frac{9BG}{3B+G} \tag{22}$$

$$\sigma=\frac{3B-2G}{6B+2G} \tag{23}$$

From Tab. 2, we can see that our calculated aggregate elastic moduli (B, G, E) are agree well with previous theoretical data[13,14], and all the elastic moduli (B, G, E) increase monotonically with increasing pressure (Fig. 5). Furthermore, according to the ratio of the bulk modulus to the shear modulus B/G, one can estimate the toughness and the brittleness of a crystal. If $B/G<1.75$, the material behaves brittleness, otherwise behaves toughness[33]. Our calculated B/G (1.34) is coincide with the value (1.39) of Yan *et al.*[14], and the data reveals the P$\bar{6}$m2-ReB_3 to be a brittle material.

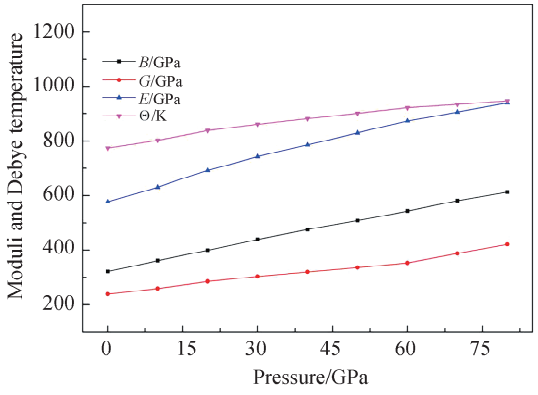

Fig. 5　Bulk modulus B, shear modulus G, Young's modulus E, and Debye temperature Θ as a function of pressure for P$\bar{6}$m2-ReB_3

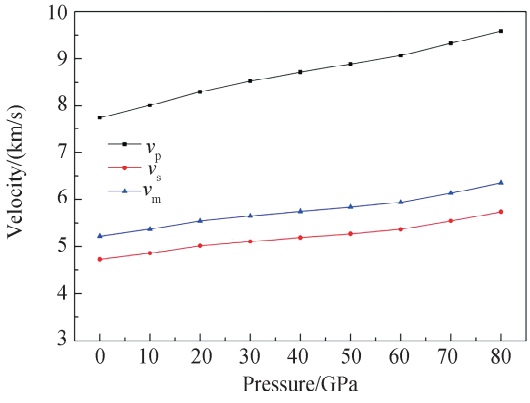

Fig. 6　Pressure dependences of aggregate velocities (v_p, v_s, v_m) for the P$\bar{6}$m2-ReB_3 structure

To complete the elastic properties of P$\bar{6}$m2-ReB_3, we also compute the compressional wave velocity v_p and shear wave velocity v_s through the Navier's equations[34]:

$$v_p=\sqrt{\left(B+\frac{4}{3}G\right)/\rho} \tag{24}$$

$$v_s=\sqrt{G/\rho} \tag{25}$$

where ρ is the density. Fig. 6 illustrates all the

velocities increase gradually with increasing pressure.

3.3 Thermodynamic properties

It is generally acknowledged that the Debye-temperature Θ is a necessary physical parameter and strongly linked to the elastic constants, melting temperature, thermal expansion coefficient, specific heats, and so on. The Debye temperature Θ can be deduced by using the following formula[35]:

$$\Theta=\frac{h}{k}\left(\frac{3n}{4\pi}\left(\frac{N_A\rho}{M}\right)\right)^{1/3}v_m \tag{26}$$

where v_m is the averaged sound velocity, and can be written as:

$$v_m=\left[\frac{1}{3}\left(\frac{2}{v_s^3}+\frac{1}{v_p^3}\right)\right]^{-1/3} \tag{27}$$

As seen in Tab. 2, our obtained Debye temperature Θ of P$\bar{6}$m2-ReB_3 at 0 GPa (773 K) is close to the theoretical reference value (764 K)[14]. Also, the Debye temperature Θ and the averaged sound velocity increase gradually with increasing pressure (Fig. 5 and Fig. 6, respectively).

In Fig. 7, the normalized volumes V/V_0 of P$\bar{6}$m2-ReB_3 are plotted versus the pressure at several temperatures (200, 500, 800 K). Obviously, the V/V_0 decreases with the increasing pressure at given temperature and decreases with the increasing temperature at given pressure. The effect of pressure on the normalized volume is similar to the effect of temperature. Fig. 8 presents the pressure dependence of bulk modulus B at given temperatures (200, 500, 800 K) for P$\bar{6}$m2-ReB_3. It is noted that the B increases with the increasing pressure at given temperature but decreases with the increasing temperature at given pressure. The effects of pressure and temperature on bulk modulus are opposite. The thermal expansion coefficient α as a function of pressure and of temperature for P$\bar{6}$m2-ReB_3 are illustrated in Fig. 9. We can see that the α decreases monotonically with the increasing pressure at all given temperatures (Fig. 9a), so it can be concluded that the effect of temperature on the pressure dependence of α is small. Meanwhile, it is noted in Fig. 9b that, at 0 GPa, α increases exponentially with T at low temperatures and increases linearly with T at high temperatures. However, when the pressure increases, the change of α with T becomes smaller, in especial at high temperatures, so we can conclude the effect of pressure on the temperature dependence of α is great at high temperatures.

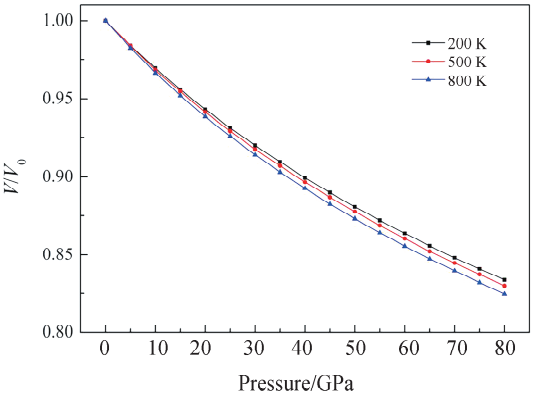

Fig. 7 The curves of normalized volume V/V_0 vs pressure for the P$\bar{6}$m2-ReB_3 structure

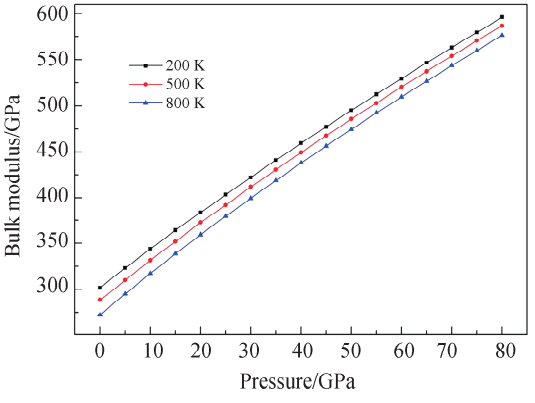

Fig. 8 Dependences of the bulk modulus B on pressure for P$\bar{6}$m2-ReB_3 at 200, 500, and 800 K, respectively

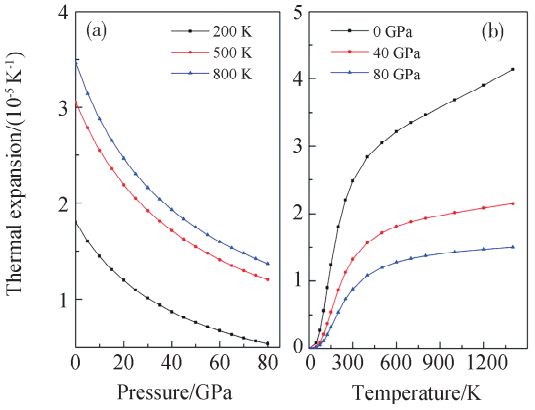

Fig. 9 The thermal expansion coefficients α of P$\bar{6}$m2-ReB_3 at various pressures and temperatures

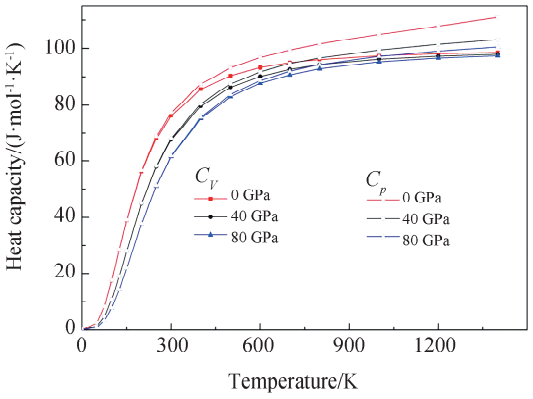

Fig. 10　The heat capacities C_V and C_p at different temperatures and pressures for the P$\bar{6}$m2-ReB_3 structure

In Fig. 10, we present the variations of the heat capacity C_V and C_p with temperature at different pressures (0, 40, 80 GPa). Clearly, the C_p approaches to C_V at low temperatures, but the differences become significantly at high temperatures. The C_V approaches to a limit while the C_p continues rising slowly with the increase of temperature. This result can be well elucidated by the Debye model. The anharmonic approximations lead to the sensitivity to temperature and pressure for C_V at low temperature. However, the anharmonic effect is suppressed for C_V at high temperature, which make the C_V approach to the Dulong-Petit limit. Besides, it can be noted that the effect of temperature on the heat capacity (C_V or C_p) is greater than that of pressure.

4　Conclusions

In summary, from our calculations, the structural, elastic and the thermodynamic properties of ReB_3 under high pressure are predicted. By observing the enthalpy difference-pressure diagram, we can predict the P$\bar{6}$m2-ReB_3 to be the ground-state phase. Moreover, the elastic constants, aggregate moduli, Debye temperatures, and aggregate wave velocities of P$\bar{6}$m2-ReB_3 are all found to increase as the pressure rises. The analysis reveals the P$\bar{6}$m2-ReB_3 to behave in brittleness. According to the curve of elastic anisotropic parameters with pressure, we can deduce the P$\bar{6}$m2-ReB_3 to be elastic anisotropy under high pressure. Furthermore, dependences of the Debye temperature, normalized volume, bulk modulus, thermal expansion coefficient and heat capacity on pressure or temperature have suggested that the pressure and temperature are closely connected with the thermodynamic properties of ReB_3.

References:

[1] Zhao E, Wu Z. Electronic and mechanical properties of 5d transition metalmononitrides via first principles [J]. J Solid State Chem, 2008, 181: 2814.

[2] Gu Q, Krauss G, Steurer W. Transition metal borides: superhard versus ultra-incompressible [J]. Adv Mater, 2008, 20: 3620.

[3] Ivanovskii A L. Microhardness of compounds of rhenium with boron, carbon, and nitrogen [J]. J Superhard Mater, 2012, 34: 75.

[4] Suetin D V, Shein I R. Electronic structure, mechanical and dynamical stability of hexagonal subcarbides M_2C(M= Tc, Ru, Rh, Pd, Re, Os, Ir, and Pt): *ab initio* calculations [J]. Phys Solid State, 2018, 60: 213.

[5] Jeanloz R, Godwal B K, Meade C. Static strength and equation of state of rhenium at ultra-high pressures [J]. Nature, 1991, 349: 687.

[6] Vohra Y K, Duclos S J, Ruoff A L. High-pressure x-ray diffraction studies on rhenium up to 216 GPa (2.16 Mbar) [J]. Phys Rev B, 1987, 36: 9790.

[7] Zhao Z, Bao K, Li D, *et al*. Nitrogen concentration driving the hardness of rhenium nitrides [J]. Sci Rep, 2014, 4: 4797.

[8] Lei H R, Zhu J, Hao Y J, *et al*. Pressure-induced structural phase transition, elastic and thermodynamic properties of ReC under high pressure [J]. Solid State Sci, 2015, 48: 49.

[9] Lei H R, Zhang L H, Li X, *et al*. Theoretical study of the elastic and the thermodynamic properties of Re_2C under high pressure [J]. J Korean Phys Soc, 2019, 74: 1004.

[10] Aronsson B, Stenberg E, Åselius J. Borides of rhenium and the platinum metals-the crystal structure of Re_7B_3, ReB_3, Rh_7B_3, $RhB_{\sim 1.1}$, $IrB_{\sim 1.1}$ and PtB [J]. Acta Chem Scand, 1960, 14: 733.

[11] Gou H, Wang Z, Zhang J, *et al*. Structural stability and elastic and electronic properties of rhenium borides: first principle investigations [J]. Inorg Chem, 2008, 48: 581.

[12] Zhao E, Wang J, Meng J, *et al*. Phase stability and

mechanical properties of rhenium borides by first-principles calculations [J]. J Comput Chem, 2010, 31: 1904.

[13] Zhao X, Nguyen M C, Wang C Z, *et al*. New stable Re-B phases for ultra-hard materials [J]. J Phys: Condens Matter, 2014, 26: 455401.

[14] Yan Q, Wang Y X, Wang B, *et al*. The ground-state structure and physical properties of ReB_3 and IrB_3 predicted from first principles [J]. RSC Adv, 2015, 5: 25919.

[15] Louail L, Maouche D, Roumili A, *et al*. Calculation of elastic constants of 4d transition metals [J]. Mater Lett, 2004, 58: 2975.

[16] Segall M D, Lindan P J D, Probert M J, *et al*. First-principles simulation: ideas, illustrations and the CASTEP code [J]. J Phys: Condens Matter, 2002, 14: 2717.

[17] Vanderbilt D. Soft self-consistent pseudopotentials in a generalized eigenvalue formalism [J]. Phys Rev B, 1990, 41: 7892.

[18] Perdew J P, Chevary J A, Vosko S H, *et al*. Atoms, molecules, solids, and surfaces: applications of the generalized gradient approximation for exchange and correlation [J]. Phys Rev B, 1992, 46: 6671.

[19] Perdew J P, Burke K, Ernzerhof M. Generalized gradient approximation made simple [J]. Phys Rev Lett, 1996, 77: 3865.

[20] Monkhorst H J, Pack J D. Special points for Brillouin-zone integrations [J]. Phys Rev B, 1976, 13: 5188.

[21] Wallace D C. Thermodynamics of crystals [M]. New York: Wiley, 1972.

[22] Wang J, Li J, Yip S, *et al*. Mechanical instabilities of homogeneous crystals [J]. Phys Rev B, 1995, 52: 12627.

[23] Barron T H K, Klein M L. Second-order elastic constants of a solid under stress [J]. Proc Phys Soc, 1965, 85: 523.

[24] Blanco M A, Francisco E, Luaña V. GIBBS: isothermal-isobaric thermodynamics of solids from energy curves using a quasi-harmonic debye model [J]. Comput Phys Commun, 2004, 158: 57.

[25] Zhu H Z, Hao Y J, Zhang L, *et al*. First principles study on the physical properties of TiB_2 under high temperature and high pressure [J]. J Sichuan Univ: Nat Sci Ed(四川大学学报：自然科学版), 2019, 56: 1105(in Chinese).

[26] Han X, Wang P P, Li D, *et al*. Theoretical study on phase transformation and thermodynamic properties of GaN [J]. J Sichuan Univ: Nat Sci Ed(四川大学学报：自然科学版), 2018, 55: 1036(in Chinese).

[27] Li J H, Sun Q, Zheng X R, *et al*. Structure, equation of states, elastic and thermal properties of YbB_6 crystal: first-principles calculations [J]. J Sichuan Univ: Nat Sci Ed(四川大学学报：自然科学版), 2020, 57: 352(in Chinese).

[28] Birch F. Finite elastic strain of cubic crystals [J]. Phys Rev, 1947, 71: 809.

[29] Lei H R, Zhu J, Hao Y J, *et al*. Theoretical study of electronic structure, phase transition, elastic, and thermodynamic properties of ReN [J]. Physica B, 2015, 458: 124.

[30] Steinle-Neumann G, Stixrude L, Cohen R E. First-principles elastic constants for the hcp transition metals Fe, Co, and Re at high pressure [J]. Phys Rev B, 1999, 60: 791.

[31] Rached H, Rached D, Benalia S, *et al*. First-principles study of structural stabilities, elastic and electronic properties of transition metal monocarbides (TMCs) and mononitrides (TMNs) [J]. Mater Chem Phys, 2013, 143: 93.

[32] Hill R. The elastic behaviour of a crystalline aggregate [J]. Proc Phys Soc A, 1952, 65: 349.

[33] Pugh S F. XCII. Relations between the elastic moduli and the plastic properties of polycrystalline pure metals [J]. Philos Mag, 1954, 45: 823.

[34] Schreiber E, Anderson O L, Soga N. Elastic constants and their measurements [M]. New York: McGraw-Hill, 1974.

[35] Anderson O L. A simplified method for calculating thedebye temperature from elastic constants [J]. J Phys Chem Solids, 1963, 24: 909.

引用本文格式：

中　文：雷慧茹，张立宏. $P\bar{6}m2$-ReB_3的高压物性研究[J]. 四川大学学报：自然科学版，2022，59：014004.

英　文：Lei H R, Zhang L H. High-pressure physical properties for $P\bar{6}m2$-ReB_3[J]. J Sichuan Univ: Nat Sci Ed, 2022, 59: 014004.